Arabian Journal of Geosciences (2019) 12: 185
https://doi.org/10.1007/s12517-019-4371-7

ORIGINAL PAPER

Using tritium and radiocarbon to determine groundwater age and delineate the flow regime in the Taiyuan Basin, China

Chunyan Guo [1,2] · Jiansheng Shi [1] · Zhaoji Zhang [1] · Fenge Zhang [1]

Received: 3 September 2018 / Accepted: 22 February 2019 / Published online: 7 March 2019

Abstract

Tritium (^{3}H) and radiocarbon (^{14}C) were used to determine the age, to delineate a flow regime, and to estimate flow velocity of medium-depth groundwater (50–200 m) from a Middle and Upper Pleistocene confined aquifer. Young groundwater age was determined using ^{3}H and an exponential piston-flow model (EPM). Three correction models (Tamers, Pearson, and Fontes and Garnier) were chosen to date the ^{14}C age of old groundwater. Groundwater ages of the medium-depth groundwater ranged from 3.5–25,790 a. Groundwater is relatively young in most of the piedmont area, although two high-age zones (with ages > 20,000 a) exist in the center of the plain. Groundwater age distribution characteristics indicated that groundwater flows from the mountain area to the basin area, and that the oldest groundwater in each high-age zone flows toward the depression cones. Two large local flow systems were formed because of overexploitation, and the regional flow system from north to south no longer exists. This study delineated the age of medium-depth groundwater in the entire Taiyuan Basin for the first time. The results can help promote the sustainable use of groundwater in the Taiyuan Basin.

Keywords Tritium · Radiocarbon · Age dating · Flow regime

Introduction

The Taiyuan Basin is a typical Cenozoic rift basin, located in Shanxi Province, northern China. Groundwater is the principal water resource for water supply in the Taiyuan Basin area. As a result of economic development and population growth, water demand has risen sharply. Overexploitation of groundwater has caused many environmental and geological problems, such as regional decline in groundwater levels, the formation of depression cones, and groundwater quality deterioration (Wu 2018; Zhang 2009). This has increased concerns regarding groundwater supply security and sustainability. These problems have a close relationship with the complex hydrogeological setting, changes in recharge amounts, and long groundwater residence times. Some regional hydrogeological surveys have previously been done in the Taiyuan Basin. Their focus was on geochemical evolution, and recharge and flow paths in the karst groundwater system of the mountain areas (Liao et al. 2014; Ma et al. 2011; Qiao et al. 2015; Sun et al. 2016). Because of the unique topography, geomorphologic features, and aquifer structures, the groundwater in the Taiyuan Basin is rich in fluoride and iodine (Guo et al. 2007a; Li et al. 2011; Tang et al. 2013). Human activities have increased the contamination of groundwater by arsenic and other pollutants (Guo et al. 2007b; Liao et al. 2014). The previous work paid little attention to groundwater age, recharge, and the flow regime of the Quaternary System in the basin area. Although Li et al. (2006) analyzed the hydrochemical characteristics of different groundwater systems and evaluated the recharge ratio of karst groundwater and fissure water using the Sr and Na balance method, the flow pattern and storage were not studied in detail. The

Handling editor: Lassaad Dassi

✉ Fenge Zhang
sistercarrie@live.cn

Chunyan Guo
ihegchunyan@163.com

Jiansheng Shi
tiger7886@263.net

Zhaoji Zhang
zhaoji99@263.net

[1] Institute of Hydrogeology and Environmental Geology, Chinese Academy of Geological Sciences, Shijiazhuang 050061, Hebei, China

[2] China University of Geosciences (Beijing), Beijing 100083, China

present study intends to address these knowledge gaps by providing new insights into the flow regime and flow rates using groundwater age-dating methods.

Groundwater age dating is informative and effective for delineating recharge areas, estimating flow velocities and recharge rates, and describing flow characteristics (Cao et al. 2018; Chen et al. 2011; Gardner and Heilweil 2014; Kamtchueng et al. 2015; Liu et al. 2014; Mcmahon et al. 2010). Groundwater age can also be used to map groundwater renewability and to describe resource attributes, thus facilitating the sustainable use of groundwater resources (Huang et al. 2017; Zhai et al. 2013; Zhang et al. 2017). Radiocarbon (^{14}C) and tritium (^{3}H) are important radioactive isotopes for groundwater dating. The ^{3}H isotope is often used for determining whether "modern" recharge exists, while ^{14}C is suited for dating old groundwater. The combination of ^{3}H and ^{14}C enables an accurate determination of groundwater age in regional aquifers. Estimating the ^{14}C age of groundwater is difficult because of factors such as dead-C dilution, mixing along the flow path, and carbon mass transfer (Geyh 2000). Therefore, ^{14}C dating of groundwater should be corrected by several models and combined with more information from the hydrogeological setting. Many models have been proposed to carry out the correction (Fontes and Garnier 1979; Kalin 2000; Mook 1976; Pearson and Hanshaw 1970; Tamers 1975; Vogel 1970). No single method can accurately estimate ^{14}C age, and thus, additional field samples should be taken, especially in recharge areas, to ensure that the groundwater age is determined as accurately as possible.

In this study, ^{3}H and ^{14}C were combined to date the age of medium-depth groundwater (50–200 m) in the Taiyuan Basin. The flow regime and velocity of the medium-depth groundwater were then delineated using groundwater age.

Study area

General description

The Taiyuan Basin (36° 50′–38° 15′ N, 111° 15′–113° 15′ E) lies in northern China, and covers an area of about 6000 km^2. It is surrounded by the Lvliang Mountains in the west and by the Taihang Mountains in the east (Fig. 1). The climate is continental semi-arid, with a mean annual temperature of 9.75 °C. The mean annual precipitation ranges from 259.8 to 655.0 mm, and is high in the mountains and low in the basin area. The area is dominated by the Asia summer monsoon, and more than 58.4% of the annual precipitation falls in the rainy season (June–September). The Fen River is the main river of the Taiyuan Basin, and extends from north to south throughout the entire length of the center of the basin.

Geological and hydrogeological setting

The Taiyuan Basin is a typical Cenozoic fault basin, and has an asymmetrical hydrogeological structure. The thicknesses of the Cenozoic sediments range from 50 to 3800 m. In the geological history of the area, the Lvliang Mountains rose dramatically, and alluvial-pluvial sediment developed in the western part of the Taiyuan Basin. There are different scales of loess hills and platforms between the mountains and the plains. Bedrock in the mountain areas consists of Cambrian–Ordovician carbonate rocks, Carboniferous–Permian coal-bearing strata, and Triassic clastic rocks (Fig. 1). As a result, the groundwater system in and around the Taiyuan Basin comprises pore groundwater systems in loose sediments, karst groundwater systems in carbonate rocks, and fissure groundwater systems in clastic rocks. The Quaternary aquifer in the basin area can be vertically divided into four groups (Fig. 2): Holocene phreatic aquifer (shallow groundwater, 0–50 m); Middle and Upper Pleistocene confined aquifer (medium-depth groundwater, 50–200 m); Lower Pleistocene confined aquifer (deep groundwater, 200–400 m); and a Tertiary confined aquifer. The medium-depth groundwater aquifer (50–200 m) is the main resource that is exploited.

The medium-depth groundwater flow direction is controlled by the terrain, and groundwater moves laterally from the edge to the center of the basin, except in the northern part where groundwater flows out of the basin. Because of overexploitation, the natural flow characteristics have changed, and some groundwater depression cones have formed, and there is essentially no groundwater flow out of the basin. The medium-depth aquifer is mainly recharged by vertical infiltration and lateral inflows. Vertical infiltrations include precipitation, leakage from the Fen River in the piedmont area, and irrigation along the rivers. The major discharge is from human abstraction.

Methods

Sampling and measurement

In July 2014, 72 groups of groundwater were collected at depths of 50 to 200 m from wells used for domestic and agricultural purposes. The locations of the sampling points are shown in Fig. 1. Each well was pumped for about half an hour before in situ parameters were measured and groundwater was sampled. In situ parameters included water temperature, pH, dissolved oxygen (DO) concentration, oxidation-reduction potential (ORP), and electric conductivity (EC). These parameters were measured using a HACH HQ30d, Single-Input Multi-

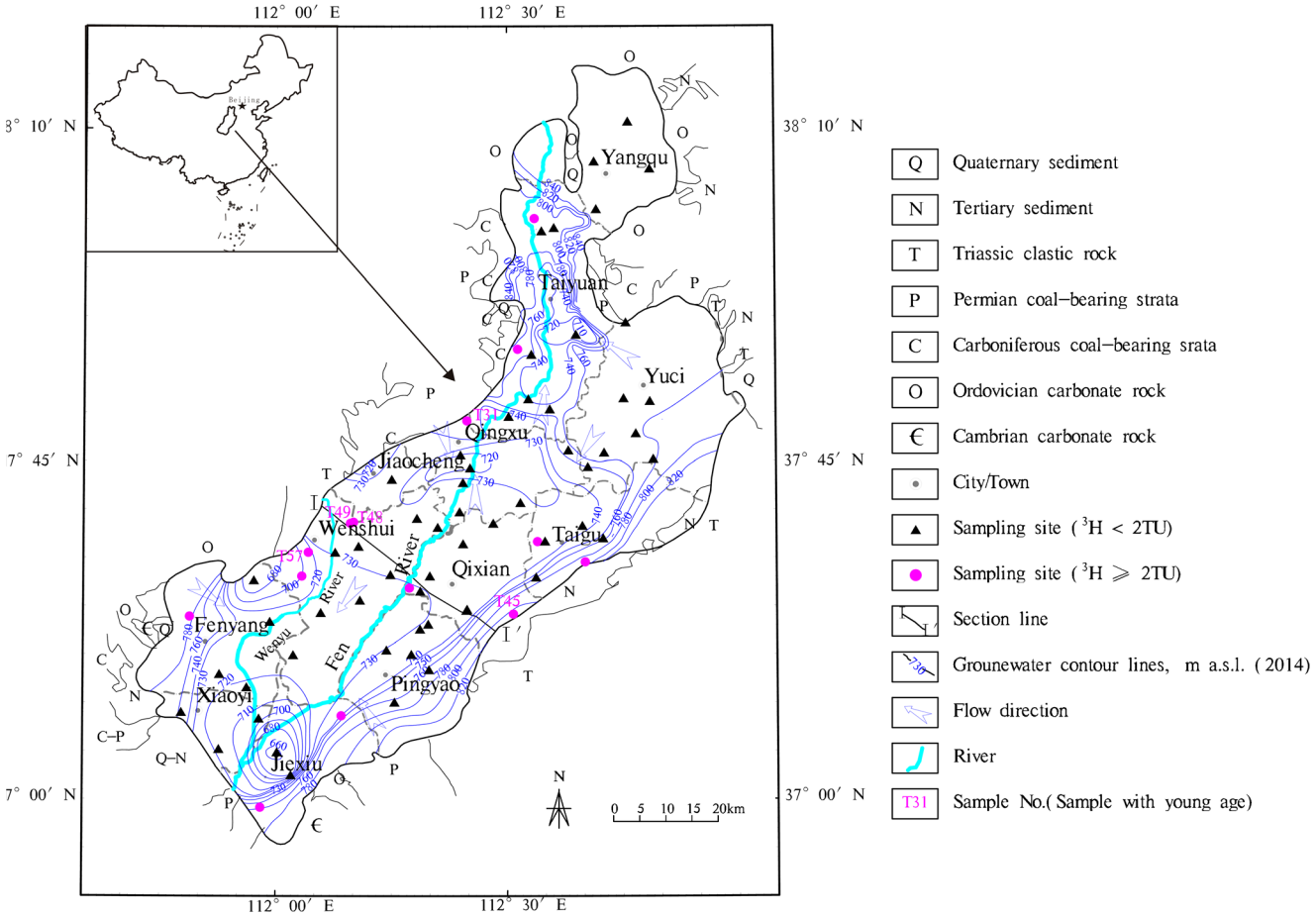

Fig. 1 Study area and sampling sites. Stratigraphic boundary around Taiyuan basin refers to Guo et al. (2007a)

Parameter Digital Meter (HACH, USA). In situ parameters were monitored until values reached a steady state. Isotope analyses (^{3}H, ^{14}C, and δ^{13}C–DIC) were carried out for each sample at the Laboratory of Groundwater Sciences and Engineering of the Institute of Hydrogeology and Environmental Geology, Chinese Academy of Geological Sciences (IHEG-CAGS). The ^{3}H isotopes were electrolytically enriched and measured using the liquid scintillation counting method with Quantulus–1220 (Pharmacia LKB, Sweden). The results were reported in tritium units (TU), with an analytical precision of ± 1 TU. The ^{14}C isotope of dissolved inorganic carbon was determined radiometrically using the liquid scintillation counting method (with the Quantulus–1220) after synthesis to benzene. The specific ^{14}C activity was reported in units of percentage modern carbon (pMC). The δ^{13}C–DIC isotopes were measured on a mass spectrometer (Finnigan MAT253, Finnigan, Germany). The results for δ^{13}C–DIC were reported as ‰ deviation from the Vienna Peedee Belemnite (VPDB, 0‰) with an analytical precision of ± 0.1‰.

Tritium model

Mathematically, the transport of ^{3}H in a hydrogeological system can be best described by the following convolution integral (Chatterjee et al. 2018; Maloszewski and Zuber 1982):

$$C_{out}(t) = \int_0^{\infty} C_{in}\left(t-t'\right) g\left(t'\right) \exp\left(-\lambda t'\right) dt' \quad (1)$$

where $Cout(t)$ is the output concentration of ^{3}H at time t(TU), C_{in} is the input concentration of ^{3}H (TU), $g(t')$ is the transit time distribution function, t is the time of sampling (a); t' is the lag time between output and input tracer composition (a), and λ is the radioactive decay constant of ^{3}H (λ=0.55764 a^{-1}).

Models commonly used in hydrogeological studies are (Cartwright and Morgenstern 2016; Maloszewski and Zuber 1982) piston-flow model (PFM), exponential mixing model (EMM), exponential piston-flow model (EPM), partial exponential model (PEM), and dispersion model (DM). Of these

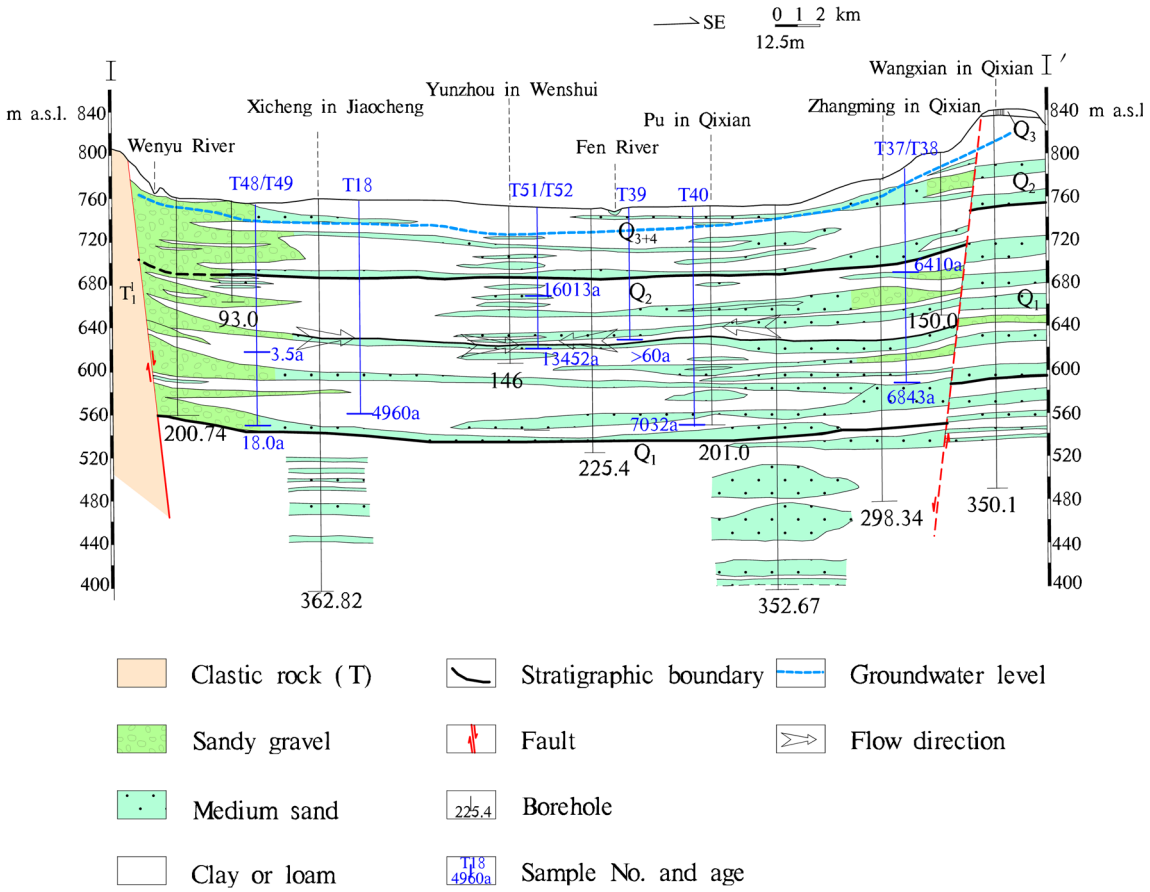

Fig. 2 Hydrogeological cross section along the I–I′ line and groundwater ages. Lithologic features originated from the China Geological Survey project (No. 200310400008)

models, the EPM is the most appropriate model for the study area because it considers flow in both horizontal and vertical directions. Each model has a different mathematical form for the transit time distribution function $g(t')$. The $g(t')$ for the EPM model is as follows (Cartwright and Morgenstern 2016):

$$g(t') = 0, \quad t' < (1-1/\eta)t_m' \tag{2a}$$

$$g(t') = (\eta/t_m')\exp(-\eta t'/t_m' + \eta - 1), \quad t' \geq (1-1/\eta)t_m' \tag{2b}$$

where t_m' is the transit time (a) and η is the ratio of the total volume to the exponential volume.

The lumped parameter method can provide estimates of the unknown parameters in the above transit time distribution function by calibrating simulations to fit the measured ^{3}H output composition (Chatterjee et al. 2018; Hagedorn et al. 2018; Jurgens et al. 2016). This is accomplished by numerically integrating the convolution integral (Eq. (1)) in the time domain. The computer code FLOWPC (Maloszewski and Zuber 1996) has been used for evaluating the mean transit time of groundwater in this study.

Radiocarbon model

Radiocarbon dating of dissolved inorganic carbon (DIC) in groundwater began in 1957, and continues to be used widely (Aravena et al. 1992; Han and Plummer 2016; Zhang et al. 2016). The ^{14}C age of DIC in a groundwater sample can be calculated from the half-life of ^{14}C decay, the initial ^{14}C content, and the measured amount of ^{14}C (Han and Plummer 2016):

$$t = -\frac{T_{1/2}}{\ln 2}\ln\frac{A_t}{A_0} \tag{3}$$

where t is the groundwater age (a), A_t is the measured ^{14}C of DIC (pMC), A_0 is initial ^{14}C (pMC), and $T_{1/2}$ is the half-life of ^{14}C ($T_{1/2}$ = 5730 a).

The theoretical principles behind the ^{14}C age calculation begin with dissolved CO_2 in precipitation entering the top soil with an initial content of 100 pMC. Then, influenced by complex geochemical and physical processes along the flow path, A_0 is altered. Thus, A_0 activity needs to be determined by a geochemical model that accounts for various sources and sinks of inorganic carbon.

Table 1 Analytical results for groundwater samples in Taiyuan Basin

Sample no.	well depth (m)	^{3}H (TU)	^{14}C (pMC)	$\delta^{13}C$–DIC (‰)	Temperature (°C)	pH
T01	200	1	7.22	16.40	16.40	7.56
T02	63	< 1.0	22.48	14.40	14.40	7.61
T03	70	4.6	33.62	20.50	20.50	7.50
T04	100	< 1.0	34.24	18.00	18.00	7.41
T05	100	< 1.0	24.92	15.40	15.40	7.63
T06	156	1.6	51.46	15.30	15.30	7.23
T07	200	1.1	24.28	16.40	16.40	7.30
T08	150	1.5	16.88	18.30	18.30	7.55
T09	110	2.5	29.83	15.80	15.80	7.54
T10	120	2.2	39.68	16.30	16.30	7.49
T11	200	< 1.0	11.02	20.70	20.70	7.76
T12	150	< 1.0	19.44	18.20	18.20	7.71
T13	200	< 1.0	7.39	19.30	19.30	7.88
T14	120	< 1.0	11.59	18.60	18.60	7.72
T15	200	< 1.0	17.06	18.40	18.40	7.62
T16	152	1.2	12.28	19.20	19.20	7.63
T17	100	1.2	14.68	17.10	17.10	7.45
T18	200	< 1.0	27.41	16.90	16.90	7.88
T19	160	< 1.0	45.42	13.60	13.60	8.12
T20	160	< 1.0	4.44	14.60	14.60	7.78
T21	200	1.4	38.16	14.20	14.20	7.55
T22	135	< 1.0	6.03	15.80	15.80	8.30
T23	200	1.7	28.34	16.20	16.20	7.87
T24	100	2.3	49.88	14.90	14.90	7.87
T25	120	2	42.26	13.80	13.80	7.62
T26	130	< 1.0	25.08	15.80	15.80	7.90
T27	100	< 1.0	44.84	24.20	24.20	7.95
T28	120	1.5	23.66	13.70	13.70	7.93
T29	150	1	19.17	17.50	17.50	7.81
T30	130	5.8	29.38	18.50	18.50	7.29
T31	100	6.7	39.1			7.36
T32	198	1.7	24.66	12.20	12.20	7.68
T33	200	< 1.0	22.95	13.90	13.90	7.74
T34	200	1.1	7.95	17.30	17.30	7.71
T35	120	1.9	15.07	14.80	14.80	7.49
T36	150	< 1.0	22.17	15.50	15.50	7.51
T37	200	< 1.0	21.42	18.90	18.90	7.95
T38	100	< 1.0	20.44	16.10	16.10	7.94
T39	120	2.3	41.96	23.30	23.30	7.70
T40	200	< 1.0	47.09	14.30	14.30	7.47
T41	200	< 1.0	28.33	18.50	18.50	7.94
T42	200	< 1.0	8.52	16.40	16.40	7.80
T43	200	< 1.0	19.2	20.50	20.50	7.94
T44	110	2.5	28.54	20.80	20.80	7.79
T45	128	8.3	75.76	17.60	17.60	7.60
T46	140	1.4	21.41	22.90	22.90	7.71
T47	175	< 1.0	11.68	20.50	20.50	8.04
T48	200	10.5	75.01	15.00	15.00	8.28
T49	130	13.5	67.46	16.70	16.70	7.92

Table 1 (continued)

Sample no.	well depth (m)	^{3}H (TU)	^{14}C (pMC)	δ^{13}C−DIC (‰)	Temperature (°C)	pH
T50	180	< 1.0	32.83	16.80	16.80	8.81
T51	155	< 1.0	7.34	15.00	15.00	7.76
T52	130	< 1.0	20.65	15.30	15.30	7.63
T53	120	< 1.0	14.89	16.40	16.40	7.74
T54	80	< 1.0	8.31	15.90	15.90	7.16
T55	165	< 1.0	9.06	15.90	15.90	7.84
T56	130	< 1.0	14.19	15.60	15.60	7.73
T57	120	7.8	37.46	17.30	17.30	7.03
T58	120	2.7	21.18	15.00	15.00	7.47
T59	190	< 1.0	5.66	17.60	17.60	8.07
T60	180	< 1.0	15.67	17.90	17.90	7.81
T61	185	< 1.0	19.16	19.10	19.10	7.63
T62	180	< 1.0	14.3	19.80	19.80	7.64
T63	200	< 1.0	12.61	15.90	15.90	7.61
T64	200	< 1.0	8.31	22.3	22.3	7.47
T65	180	< 1.0	6.01	22.1	22.1	7.69
T66	200	1.1	11.07	17.7	17.7	7.36
T67	200	< 1.0	18.22	16.9	16.9	7.46
T68	160	< 1.0	26.45	14.9	14.9	7.69
T69	130	1.3	3.23	13.6	13.6	7.67
T70	200	1.3	43.74	13.9	13.9	7.74
T71	135	< 1.0	56.24	14.7	14.7	8.16
T72	100	1.4	3.71	14.5	14.5	8.17

Results and discussion

Groundwater age dating by ^{3}H

The ^{3}H values for medium-depth groundwater ranged from < 1 to 13.5 TU (Table 1). Fourteen samples had a ^{3}H content of more than 2TU. This indicates that they are probably recharged by modern water of less than 60 a. The depths of the wells from which the samples were taken are mainly between 100 and 150 m (Fig. 3). These wells are located in the piedmont area or near the Fen River (Fig. 1). The ^{3}H ages of groundwater in the

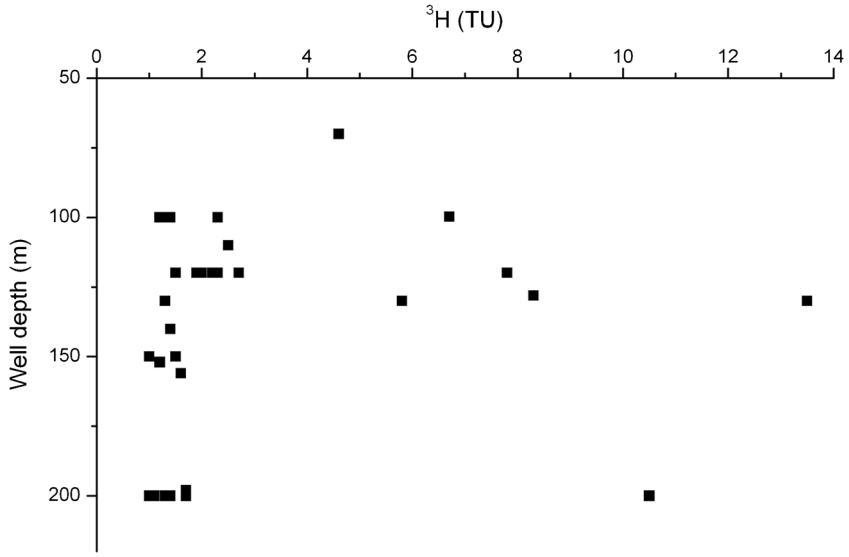

Fig. 3 The change of ^{3}H concentrations with well depth

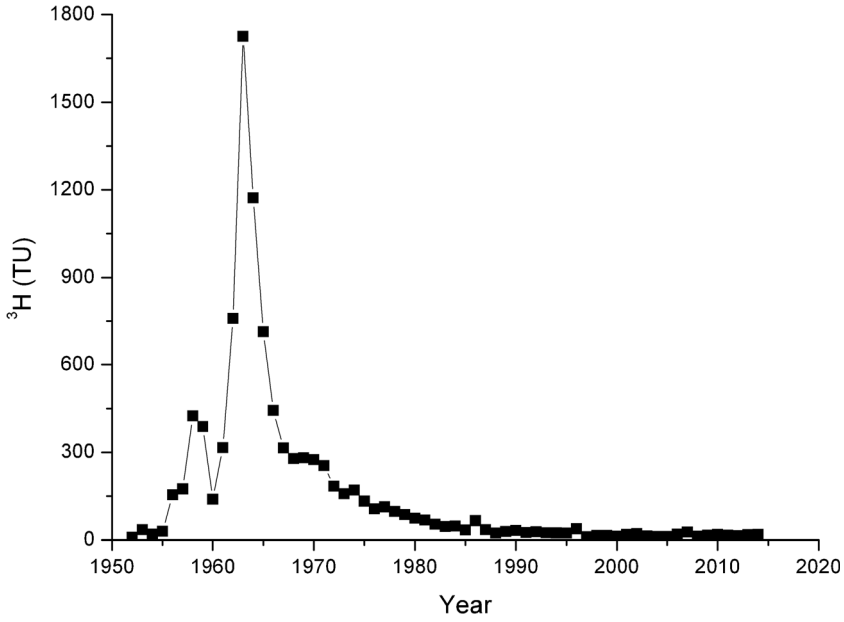

Fig. 4 ^{3}H input concentration in precipitation in the Taiyuan basin

wells were determined by using the lumped parameter method.

The calculation of groundwater age requires that the input concentration of ^{3}H in precipitation is known. However, observations of ^{3}H concentrations in precipitation in the Taiyuan Basin are only available for 1986 and 1988. Therefore, the data were reconstructed using the Doney model (Doney et al. 1992) for 1960–1986, and then corrected using monitoring data from Shijiazhuang (a city not far from Taiyuan) for the years when data were not available. The reconstructed ^{3}H input concentration in precipitation is shown in Fig. 4.

The medium-depth aquifers of the Taiyuan Basin are recharged by lateral flow from the mountain areas, and by the infiltration of surface water and shallow groundwater. Therefore, the EPM model was chosen to obtain young groundwater ages. Trial calculations were carried out by adjusting the η value and the transit time (t_m') to fit the observed ^{3}H values in 2004. The best fitting was obtained when $\eta = 7.5$, and $t_m' = 7$. These parameters were then used to obtain the ^{3}H output concentration curve (Fig. 5). The groundwater age was estimated from this curve. Final ages were determined by considering the samples' location and the hydrogeological characteristics of the area (Table 2). Most samples had ages of more than 60 a, while T31, T45, T48, T49, and T57 were recharged in recent years (Table 2 and Fig. 1). T49 is the youngest groundwater, and is located in the piedmont area

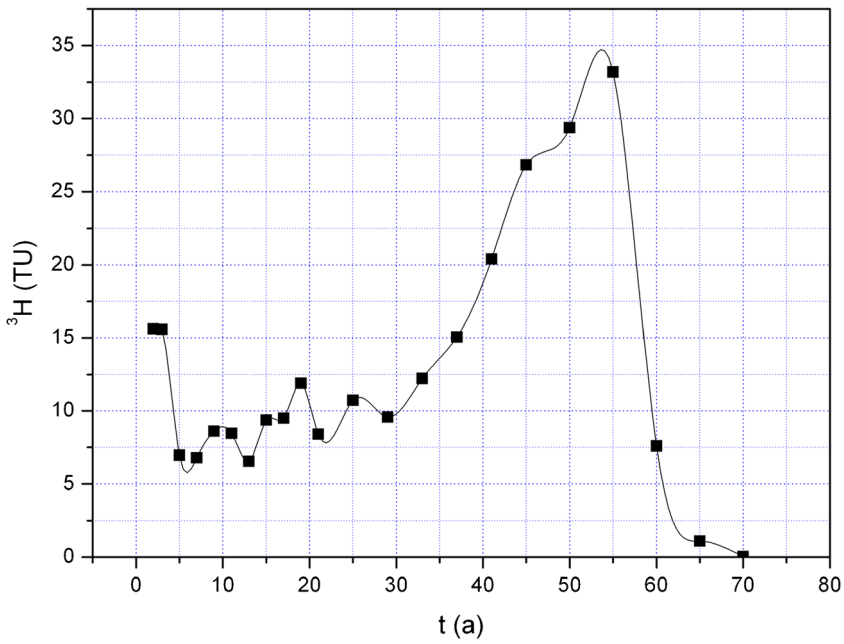

Fig. 5 ^{3}H output concentration curves from the EPM (in 2014). The curve was constructed by using the precipitation correction of the monitoring data in Shijiazhuang

Table 2 ^{3}H age calculated from EPM

Sample no.	Well depth (m)	^{3}H (TU)	EPM model age (a)	Determined age (a)
T03	70	4.6	> 60	> 60
T09	110	2.5	> 60	> 60
T10	120	2.2	> 60	> 60
T24	100	2.3	> 60	> 60
T25	120	2	> 60	> 60
T30	130	5.8	> 60	> 60
T31	100	6.7	6, 12, > 60	12
T39	120	2.3	> 60	> 60
T44	110	2.5	> 60	> 60
T45	128	8.3	8.8, 10.8, 59.5	10.8
T48	200	10.5	18, 21, 24, 26, 32, 59	18
T49	130	13.5	3.5, 35.0, 58.5	3.5
T57	120	7.8	4.5, 8.3, 11.8, 59.8	11.8
T58	120	2.7	> 60	> 60

of the single layer aquifer. Its young age is probably caused by the infiltration of surface water from the Wenyu River (Fig. 2).

Groundwater age dating by ^{14}C

The measured ^{14}C of DIC values ranged from 0.6 to 75.76 pMC, with an average of 24.27 pMC (Table 1). Samples with a high content of ^{14}C are consistent with samples with a high ^{3}H content. This shows that these samples are mixtures of modern and old water. The $\delta^{13}C$ of DIC exhibits a wide range of values (from − 20 to − 4‰) with an average of − 11.1‰ (Table 1). Based on the relationship between $\delta^{13}C$–DIC and ^{14}C (Fig. 6), two groups could be identified: group 1 (^{14}C content less than 25 pMC) with a wide range of $\delta^{13}C$–DIC values and an average of − 11.6‰ and group 2 (^{14}C content more than 25 pMC) with a wide range of $\delta^{13}C$–DIC values and an average of − 10.3‰. The differences in these groups indicate that (1) groundwater is recharged under various conditions (humid-dry, open-closed, different aquifer matrices); and (2) the geochemical evolution of some of the samples has progressed further than others, for example, in the dissolution of carbonate (Stadler et al. 2010). If it is assumed that, for a given sample pH and temperature, the soil CO_2 is in equilibrium with the $\delta^{13}C$ of DIC, then the soil CO_2 can be calculated from the $\delta^{13}C$ value of DIC. The calculated values for soil CO_2 in the recharge area ranged from − 28.6 to − 7.4‰ with an average of − 19.7‰, which reflect that the input carbon originated from C_3-plants.

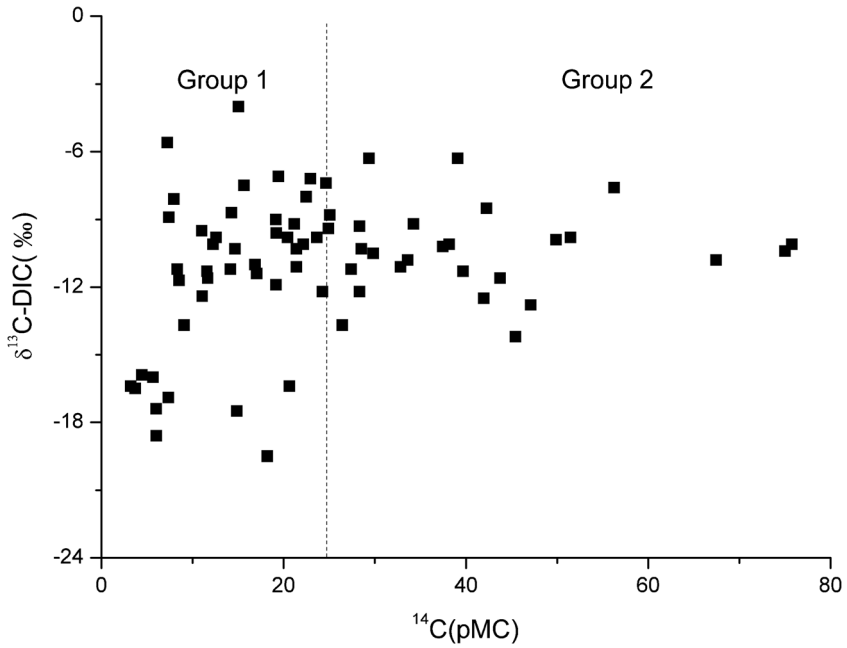

Fig. 6 Plot of ^{14}C activities of groundwater samples versus their $\delta^{13}C$–DIC values

Table 3 ^{14}C age determined by comparing various models

Sample no.	^{14}C (pMC)	$\delta^{13}C$–DIC (‰)	Corrected ^{14}C age (a)			
			Tamers	Pearson	Fontes and Garnier	Average
T01	7.22	− 5.6	16,530	10,049	Modern	13,290
T02	22.48	− 8	7106	3608	2051	4255
T04	34.24	− 9.2	3835	1285	388	1836
T05	24.92	− 9.4	6225	4090	2707	4341
T06	51.46	− 9.8	807	Modern	812	809
T07	24.28	− 12.2	6870	6460	7769	7033
T08	16.88	− 11	9503	8610	8910	9007
T11	11.02	− 9.5	12,826	10,923	9728	11,159
T12	19.44	− 7.1	8185	3823	2898	4969
T13	7.39	− 8.9	16,060	13,687	12,984	14,244
T14	11.59	− 11.3	12,451	11,940	13,181	12,524
T15	17.06	− 11.4	9343	8817	10,022	9394
T16	12.28	− 10.1	12,045	10,534	11,012	11,197
T17	14.68	− 10.3	10,791	9220	12,548	10,853
T18	27.41	− 11.2	5235	4751	4892	4960
T19	45.42	− 14.2	961	2538	4315	2604
T20	4.44	− 15.9	20,362	22,696	24,951	22,670
T21	38.16	− 10.1	2799	1161	Modern	1980
T22	6.03	− 18.6	17,593	21,462	24,434	21,163
T23	28.34	− 9.3	4969	2938	1442	3116
T26	25.08	− 8.8	5963	3492	420	3292
T27	44.84	–	1102			1102
T28	23.66	− 9.8	6439	4863	3771	5024
T29	19.17	− 11.9	8232	8208	8875	8438
T32	24.66	− 7.4	6291	2199	Modern	4245
T33	22.95	− 7.2	6818	2566	Modern	4692
T34	7.95	− 8.1	15,583	12,304	9635	12,508
T35	15.07	− 4	10,547	1184		5866
T36	22.17	− 10.1	7323	5650	5978	6317
T37	21.42	− 11.1	7228	6715	6585	6843
T38	20.44	− 9.8	7631	6073	5524	6410
T40	47.09	− 12.8	1160	1381	2643	1728
T41	28.33	− 12.2	4923	5185	6416	5508
T42	8.52	− 11.7	14,949	14,772	15,210	14,977
T43	19.2	− 9.6	8131	6420	5501	6684
T46	21.41	− 10.3	7360	6101	9337	7599
T47	11.68	− 11.6	12,197	12,093	12,664	12,318
T50	32.83	− 11.1	3510	3185	3213	3303
T51	7.34	− 16.9	16,219	19,044	21,965	19,076
T52	20.65	− 16.4	7779	10,245	12,778	10,267
T53	14.89	− 17.5	10,378	13,485	16,493	13,452
T54	8.31	–	16,013			16,013
T55	9.06	− 13.7	14,417	15,568	17,079	15,688
T56	14.19	− 11.2	10,789	10,194	10,897	10,627
T59	5.66	− 16	18,183	20,741	22,978	20,634
T60	15.67	− 7.5	9896	6058	2645	6200
T61	19.16	− 9	8369	5903	4668	6313

Table 3 (continued)

Sample no.	^{14}C (pMC)	δ^{13}C–DIC (‰)	Corrected ^{14}C age (a)			
			Tamers	Pearson	Fontes and Garnier	Average
T62	14.3	− 8.7	10,773	8042	9692	9502
T63	12.61	− 9.8	11,872	10,066	10,179	10,705
T64	8.31	− 11.2	15,247	14,617	16,108	15,324
T65	6.01	− 17.4	17,925	20,938	23,292	20,718
T66	11.07	− 12.4	12,859	13,088	16,348	14,098
T67	18.22	− 19.5	8740	12,711	15,954	12,468
T68	26.45	− 13.7	5652	6711	8597	6987
T69	3.23	− 16.4	23,031	25,582	28,769	25,794
T70	43.74	− 11.6	1516	1177	1211	1301
T71	56.24	− 7.6	Modern	Modern	Modern	Modern
T72	3.71	− 16.5	21,886	24,487	27,493	24,622

– show that δ^{13}C value is not available; Correspondingly, ^{14}C age cannot be calculated from Pearson and Fontes and Garnier without δ^{13}C value; "Modern" indicates minus values

Groundwater with a ^{3}H less than 2TU was recharged before the 1950s, and the age of these samples was determined using ^{14}C. To calculate the appropriate age of groundwater, correction models are needed to be employed. Seven models were used in this study: (1) Vogel (Vogel 1970), (2) IAEA (Mook 1976), (3) Tamers (Tamers 1975), (4) Pearson (Pearson and Hanshaw 1970), (5) Fontes and Garnier (Fontes and Garnier 1979), (6) Alkalinity (ALK) (Tamers 1975), and (7) chemical mass balance (CMB) (Kalin 2000). These models consider either chemical mixing between

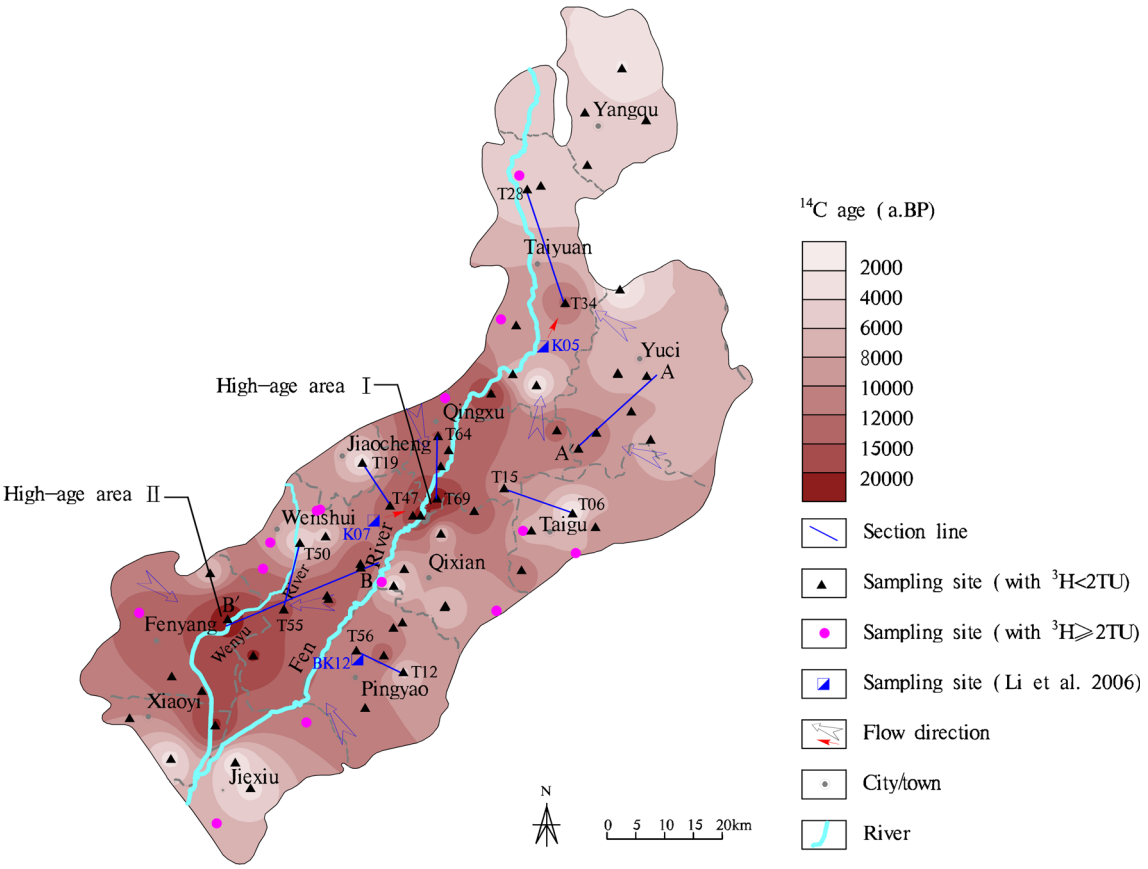

Fig. 7 The counter map of ^{14}C ages in the Taiyuan Basin and flow path sections

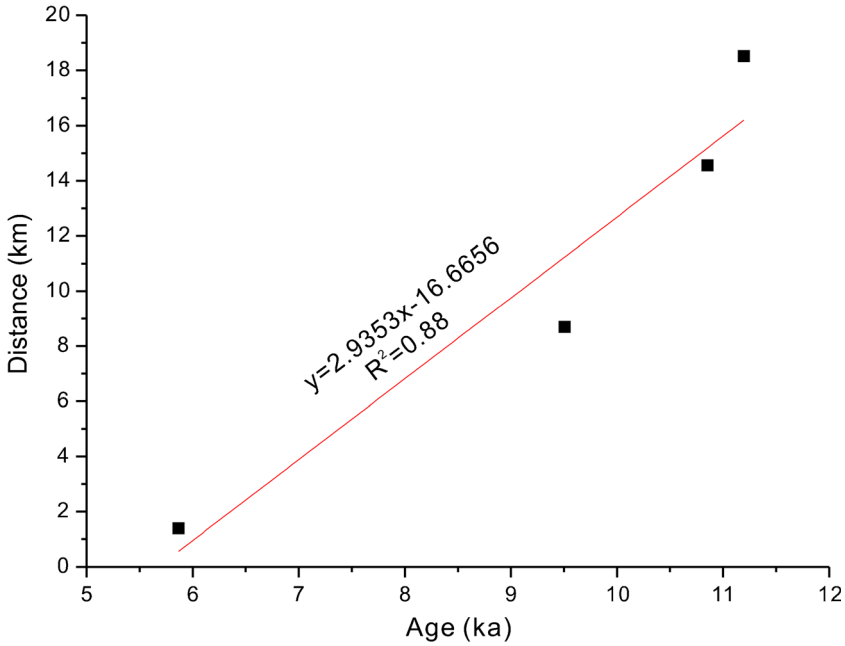

Fig. 8 Variation of groundwater age with groundwater flow path (A–A′ section)

carbon compounds and/or isotopic fractions. The samples' pH and temperature are needed in the calculation process. In addition, $\delta^{13}C$ values of soil CO_2 gas and soil carbonate (0‰) are needed for the IAEA, Pearson, and Fontes and Garnier models. The average A_0 values calculated using these models showed that the Vogel model gives the largest A_0 (80 pMC); the ALK and CMB models give very low A_0 (averages of 18.0 pMC and 24.8 pMC, respectively); the Tamer, Pearson, and Fontes and Garnier models yielded similar A_0 values (averages of 52.5 pMC, 49.8 pMC, and 53.1 pMC, respectively). The actual A_0 is therefore probably about 50 pMC. The ^{14}C age of the medium-depth groundwater was calculated from the three models. The average values from the three models were taken as the final ages (809–25,894 a) (Table 3).

Groundwater flow regime and velocity

Groundwater flow regime

The groundwater flow field was mapped from the groundwater-level data observed and collected in this study (Fig. 1). Groundwater flows from the piedmont area to the basin center area, or to the depression cones. Three large groundwater depression cones (at Taiyuan, Qingxu, and

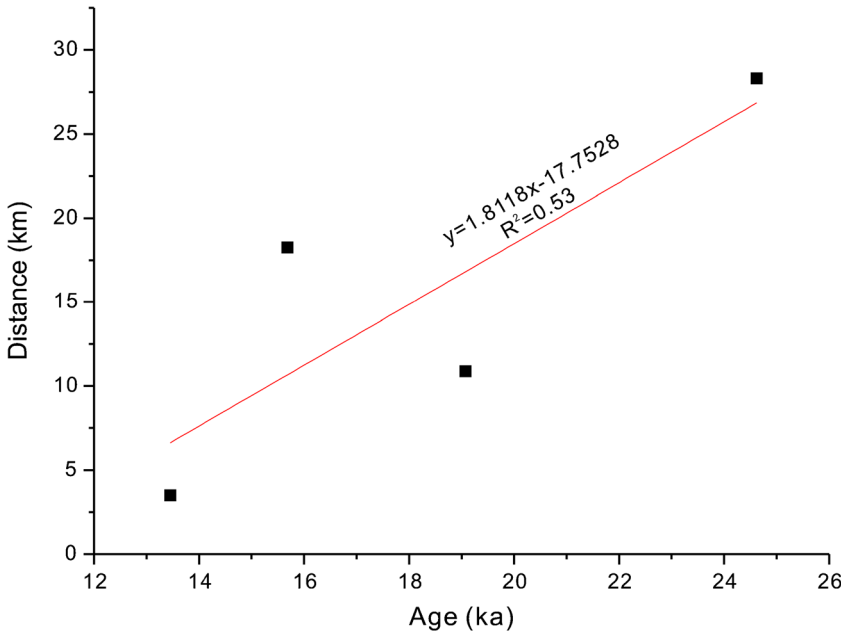

Fig. 9 Variation of groundwater age with groundwater flow path (B–B′ section)

Table 4 Representative flow velocity of groundwater in Taiyuan Basin

Location	Sample no.	^{14}C age (a)	Age difference (a)	Distance (m)	Flow velocity (m/a)
Taiyuan in northern piedmont	T28	5024.32			
	T34	12,507.68	7483.36	20,812.5	2.78
Jiaocheng in western piedmont	T19	2605			
	T47	12,318	9713	8750	0.90
Taigu in eastern piedmont	T06	809			
	T15	9394	8585	12,425	1.45
Qingxu around groundwater depression cone	T64	15,320			
	T69	25,790	10,530	10,530	1.01
Wenshui in western piedmont	T50	3303			
	T55	15,688	12,385	12,075	0.97
Pingyao in eastern piedmont	T12	4969			
	T56	10,627	5658	8375	1.48

Jiexiu) have formed in the center of the basin. Because of the groundwater depression in Qingxu, a watershed has appeared between Qiaocheng and Wenshui Counties. Thus, two large, local, groundwater flow systems were formed as the result of intensive exploitation.

Groundwater ages become older along the flow path, and thus can help to delineate the flow path and flow regime. The distribution of groundwater age as determined by ^{14}C is shown in Fig. 2 and Fig. 7, and shows that groundwater flow in the center of the basin is complex. Most of the groundwater in the piedmont area is relatively young, with ages < 10,000 a, while the groundwater in the depression cone at Taiyuan City is relatively old, with an age of 12,508 a. Two high-age zones (ages > 20,000 a) exist in the center part of the basin: one is located in the south of Qingxu (high-age area I), and the other is located in Fenyang (high-age area II) in the south of the Taiyuan Basin which was the only discharge zone for the whole basin in the past. The two high-age zones' distribution characteristics also indicate the presence of a watershed.

The direction of local groundwater flow system was identified. The flows are mainly to the high-age zones. At Taiyuan, the distribution of the high-age zone coincided with groundwater depression cone. At Qingxu and Fenyang, the two high-age zones were distributed near groundwater depression cones, and groundwater in the high-age zones showed a trend of moving toward the depression cones. These trends can be confirmed by comparing the groundwater ages determined in the present study to those determined in the study by Li et al. (2006). In Li's research, three medium-depth groundwater samples' ages were dated (K05, K07, and BK12 with ages of 17,652 a, 21,238 a, and 13,252 a, respectively). The samples' locations are shown in Fig. 7. With respect to the corresponding groundwater areas in the present study, the groundwater age at BK12 has not changed significantly since Li's study. The groundwater ages at the positions of K05 and K07 have become younger (10000–12000 a), while to their north, the groundwater ages have increased. The groundwater at sites K05 and K07 have moved toward the center of the depression cones in past years (red arrows show the direction of movement in Fig. 7). As a consequence, the oldest groundwater will be exploited in the depression cones in future if overexploitation in the depression areas continues. Once this groundwater has been used, it cannot be restored.

Groundwater flow velocity

Groundwater flow velocity, the reciprocal of the age gradient, was calculated along the flow path. Two transect sections (A–A′ and B–B′), and several segments, were chosen to estimate groundwater flow velocity. For sections A–A′ and B–B′, the mean flow velocity estimated from the slope of the fitting line (Fig. 8 and Fig. 9) was 2.94 m/a and 1.81 m/a, respectively. The groundwater velocity for the other segments is given in Table 4. The velocities of the medium-depth groundwater ranged from 0.90 to 2.94 m/a. Groundwater in the eastern part of the study area flows faster than in the western part. Groundwater in the northern and Yuci piedmont areas (with velocity of 2.78 m/a and 2.94 m/a, respectively) flow faster than in other areas. The groundwater velocity in the Jiaocheng piedmont area is slowest. On the whole, the medium-depth groundwater of the Taiyuan Basin flows slowly.

Conclusions

Radioactive isotopes ^{3}H and ^{14}C were used to date groundwater age, delineate the groundwater flow regime, and estimate the groundwater velocity of medium-depth groundwater (50–200 m) in the Taiyuan Basin. The ^{3}H values show that groundwater age ranges from 3.5 to > 60a, indicating that some groundwater was recharged by modern water and mixed with old groundwater. The ^{14}C model gave ages ranging from 809

to 25790 a. The groundwater becomes older from the piedmont area to the center of the basin. Two separate areas with old groundwater are present in the center of the basin. Groundwater flow velocity ranges from 0.90 to 2.94 m/a. Groundwater in the eastern part flows faster than in the western part. Age evolution along the flow line from the mountains to the basin is apparent, indicating recharge from the mountain areas. Two new findings that were not evident in earlier studies were obtained: a watershed has appeared in the center of the basin, and the regional north-to-south groundwater system has disappeared. Although the groundwater flow is very slow, the trend of the oldest groundwater moving to the centers of the depression cones is obvious.

Groundwater renewability can be characterized on the basis of groundwater age and flow regime, and this can provide useful information regarding the sustainable use of groundwater. Groundwater in the southern piedmont area is relatively young and some parts are recharged by modern water. Thus, there is partial groundwater renewal in this area and groundwater can be exploited appropriately here. However, the groundwater in the western piedmont area is not effectively recharged and two groundwater depression cones have formed. It is, therefore, no longer suitable for exploitation. The groundwater in the southern part of the study area (the discharge area in the past) can be exploited relatively highly, although the renewability is small. Increased exploitation here will accelerate groundwater recharge, from lateral inflows and vertical infiltration.

Acknowledgments We thank Liwen Bianji, Edanz Editing China (www.liwenbianji.cn/ac), for editing the English text of a draft of this manuscript.

Funding information This study was funded by the National Natural Science Foundation of China (No. 41502254) and the China Geological Survey project (No.12120114086401).

References

Aravena R, Warner BG, Macdonald GM, Hanf KI (1992) Carbon isotope composition of lake sediments in relation to lake productivity and radiocarbon dating. Quat Res 37(3):333–345

Cao W, Yang H, Liu C, Li Y, Bai H (2018) Hydrogeochemical characteristics and evolution of the aquifer systems of Gonghe Basin, Northern China. Geosci Front 9:907–916

Cartwright I, Morgenstern U (2016) Using tritium to document the mean transit time and sources of water contributing to a chain-of-ponds river system: implications for resource protection. Appl Geochem 75:9–19

Chatterjee S, Sinha UK, Ansari MA, Mohokar HV, Dash A (2018) Application of lumped parameter model to estimate mean transit time (MTT) of the thermal water using environmental tracer (^{3}H): insight from Uttarakhand geothermal area (India). Appl Geochem 94:1–10

Chen Z, Wei W, Liu J, Wang Y, Chen J (2011) Identifying the recharge sources and age of groundwater in the Songnen plain (northeast China) using environmental isotopes. Hydrogeol J 19(1):163–176

Doney SC, Glover DM, Jenkins WJ (1992) A model function of the global bomb tritium distribution in precipitation, 1960–1986. J Geophys Res Oceans 97(C4):5481–5492

Fontes JC, Garnier JM (1979) Determination of the initial ^{14}C activity of the total dissolved carbon: a review of the existing models and a new approach. Water Resour Res 15(2):399–413

Gardner PM, Heilweil VM (2014) A multiple-tracer approach to understanding regional groundwater flow in the snake valley area of the eastern great basin, USA. Appl Geochem 45(3):33–49

Geyh MA (2000) An overview of ^{14}C analysis in the study of groundwater. Radiocarbon 42(1):99–114

Guo Q, Wang Y, Ma T, Ma R (2007a) Geochemical processes controlling the elevated fluoride concentrations in groundwater of the Taiyuan basin, northern China. J Geochem Explor 93(1):1–12

Guo Q, Wang Y, Gao X, Ma T (2007b) A new model (DRARCH) for assessing groundwater vulnerability to arsenic contamination at basin scale: a case study in Taiyuan basin, northern China. Environ Geol 52(5):923–932

Hagedorn B, Clarke N, Ruane M, Faulkner K (2018) Assessing aquifer vulnerability from lumped parameter modeling of modern water proportions in groundwater mixtures: application to California's south coast range. Sci Total Environ 624:1550–1560

Han L, Plummer LN (2016) A review of single-sample-based models and other approaches for radiocarbon dating of dissolved inorganic carbon in groundwater. Earth Sci Rev 152:119–142

Huang T, Pang Z, Li J, Xiang Y, Zhao Z (2017) Mapping groundwater renewability using age data in the Baiyang alluvial fan, NW China. Hydrogeol J 25(3):743–755

Jurgens BC, Böhlke JK, Kauffman LJ, Belitz K, Esser BK (2016) A partial exponential lumped parameter model to evaluate groundwater age distributions and nitrate trends in long-screened wells. J Hydrol 543:109–126

Kalin RM (2000) Radiocarbon dating of groundwater systems. In: Environmental Tracers in Subsurface Hydrology. Springer US, New York

Kamtchueng BT, Fantong WY, Wirmvem MJ, Tiodjio RE, Takounjou AF, Asai K et al (2015) A multi-tracer approach for assessing the origin, apparent age and recharge mechanism of shallow groundwater in the lake Nyos catchment, northwest, Cameroon. J Hydrol 523:790–803

Li X, Hou X, Zhang H, Zhang L (2006) Study on the geochemistry-isotope characteristics of the groundwater systems in Taiyuan basin. J Arid Land Resour Environ 20(5):109–114 (In Chinese with English abstract)

Li X, Hou X, Zhou Z, Liu L (2011) Geochemical provenance and spatial distribution of fluoride in groundwater of Taiyuan basin, China. Environ Earth Sci 62(8):1635–1642

Liao Y, Ma T, Cui Y, Qi Z (2014) Spatial distribution characteristics of volatile halogenated hydrocarbons in unsaturated zone of Xiaodian sewage irrigation area, Taiyuan, China. Ecotoxicology 23(10):1951–1957

Liu J, Chen Z, Wei W, Zhang Y, Li Z, Liu F, Guo H (2014) Using chlorofluorocarbons (CFCs) and tritium (3h) to estimate groundwater age and flow velocity in Hohhot basin, China. Hydrol Process 28(3):1372–1382

Ma R, Wang Y, Sun Z, Zheng C, Ma T, Prommer H (2011) Geochemical evolution of groundwater in carbonate aquifers in Taiyuan, northern China. Appl Geochem 26(5):884–897

Maloszewski P, Zuber A (1982) Determining the turnover time of groundwater systems with the aid of environmental tracers: 1. Models and their applicability. J Hydrol 57:207–231

Maloszewski P, Zuber A (1996) Lumped parameter models for the interpretation of environmental tracer data, chap. 2 in International

Atomic Energy Agency. In: Manual on Mathematical Models in Isotope Hydrogeology, TECDOC-910

Mcmahon PB, Carney CP, Poeter EP, Peterson SM (2010) Use of geochemical, isotopic, and age tracer data to develop models of groundwater flow for the purpose of water management, northern high plains aquifer, USA. Appl Geochem 25(6):910–922

Mook WG (1976) The dissolution-exchange model for dating ground water with carbon-14. In: Interpretation of environmental isotope and hydrochemical data in ground water hydrology. IAEA, Vienna, pp 213–225

Pearson FJ, Hanshaw BB (1970) Sources of dissolved carbonate species in groundwater and their effects on carbon-14 dating. In: Isotope hydrology. IAEA, Vienna, pp 271–286

Qiao X, Li G, Li Y, Liu K (2015) Influences of heterogeneity on three-dimensional groundwater flow simulation and wellhead protection area delineation in karst groundwater system, Taiyuan city, northern China. Environ Earth Sci 73(10):6705–6717

Stadler S, Osenbrück K, Suckow AO, Himmelsbach T, Hötzl H (2010) Groundwater flow regime, recharge and regional-scale solute transport in the semi-arid Kalahari of Botswana derived from isotope hydrology and hydrochemistry. J Hydrol 388(3–4):291–303

Sun Z, Ma R, Wang Y, Ma T, Liu Y (2016) Using isotopic, hydrogeochemical-tracer and temperature data to characterize recharge and flow paths in a complex karst groundwater flow system in northern China. Hydrogeol J 24(6):1–20

Tamers MA (1975) Validity of radiocarbon dates on ground water. Surv Geophys 2(2):217–239

Tang Q, Xu Q, Zhang F, Huang Y, Liu J, Wang X, Yang Y, Liu X (2013) Geochemistry of iodine-rich groundwater in the Taiyuan basin of central Shanxi province, north China. J Geochem Explor 135(6): 117–123

Vogel JC (1970) Carbon-14 dating of groundwater. In: Isotope hydrology. IAEA, Vienna, pp 225–239

Wu S (2018) Analysis on the evolution situation of the deep groundwater level drawdown funnel in the meantime of the recent 25 years in Taiyuan. Shanxi Hydrotechnics 1:68–70 (In Chinese with English abstract)

Zhai Y, Wang J, Huan H, Zhou J, Wei W (2013) Characterizing the groundwater renewability and evolution of the strongly exploited aquifers of the north China plain by major ions and environmental tracers. Journal of Radioanalytical and Nuclear Chemistry 296(3): 1263–1274

Zhang Y (2009) Environmental impacts of groundwater utilization in Taiyuan basin. Shanxi Water Resources 6:5–6 (In Chinese)

Zhang J, Ma X, Qiang M, Huang X, Li S, Guo X, Henderson ACG, Holmes JA, Chen F (2016) Developing inorganic carbon-based radiocarbon chronologies for Holocene lake sediments in arid NW China. Quaternary Science Reviews 144:66–82

Zhang B, Song X, Zhang Y, Han D, Tang C, Yang L et al (2017) The renewability and quality of shallow groundwater in Sanjiang and Songnen plain, northeast China. Journal of Integrative Agriculture 16(1):229–238